Journal of Nuclear Materials 383 (2008) 28–33

Contents lists available at ScienceDirect

Journal of Nuclear Materials

journal homepage: www.elsevier.com/locate/jnucmat

The transformation behaviour of the β-phase in Zr–2.5Nb pressure tubes

M. Griffiths *, J.E. Winegar, A. Buyers

Atomic Energy of Canada Ltd., Chalk River, Ontario, Canada

ARTICLE INFO

PACS:
81.40.Ef
28.41.Fr

ABSTRACT

In a CANDU reactor, the fuel bundles and primary coolant are contained within Zr–2.5Nb pressure tubes that are approximately 6.3 m in length, have an internal diameter of 104 mm and a wall thickness of 4.2 mm. The Zr–2.5Nb pressure tubes are nominally extruded at 815 °C, cold-worked 27%, and stress relieved at 400 °C for 24 h, resulting in a structure consisting of elongated grains of hexagonal-close-packed α-Zr, partially surrounded by a thin network of filaments of body-centred-cubic β-Zr. These β-Zr filaments are metastable and contain about 20% Nb. The stress-relief treatment results in partial decomposition of the β-Zr filaments with the formation of hexagonal-close-packed ω-phase particles that are low in Nb, surrounded by a Nb-enriched β-Zr matrix. A temperature–time–transformation (TTT) diagram has been developed for the β-phase in Zr–2.5 wt%Nb pressure tubes. The results show that the morphology and/or physical state of the β-phase has a significant effect on the transformation behaviour compared with a bulk Zr–20 wt%Nb alloy. This means that a specific TTT-diagram is required to describe the behaviour of these engineering components.

1. Introduction

Zr–2.5Nb pressure tubes are made of Zr–2.5 wt%Nb, a material that has a low neutron absorption cross-section, a high resistance to corrosion in water, a high strength and good creep resistance. The tubes are fabricated by extruding billets at about 820 °C and then cold-working to size. During extrusion, a two-phase structure is formed that consists of hexagonal α-zirconium grains (containing up to about 1 wt%Nb) and a grain boundary network of metastable cubic β-zirconium (containing about 20 wt%Nb) corresponding with the composition at the monotectoid point of the phase diagram [1], Fig. 1(a). This metastable β-phase transforms into other phases with time at temperatures below 600 °C. For example, the final stress-relief treatment in an autoclave for the tubes is 24 h at 400 °C, and it partially decomposes the β-phase relative to the as-extruded state, Fig. 1(b). A hcp ω-phase is formed that is depleted in the β-stabilising elements, Nb and Fe, with a subsequent enrichment of these elements in the remaining β-phase. X-ray diffraction (XRD) can be used to detect the phases present and to determine their composition. The exact angular position of the peaks is determined by the crystal structure, chemical composition (variable in some cases), and the residual stress within the phase.

The equilibrium monotectoid composition of the β-phase should be about 20 wt%Nb, based on information from the zirconium–niobium equilibrium phase diagram [1]. In an earlier study [2,3], an alloy of Zr–19 wt%Nb was used to study the age-hardening, tensile, and transformation behaviour of the β-phase. However, recent work has shown that the transformation behaviour of the β-phase in actual pressure tube material differed in some instances from that of the model alloy. Therefore, this study has been conducted using pressure tube material to determine the time–temperature–transformation (TTT) characteristics of the β-phase. One disadvantage to using pressure tube material is that the α-phase is always the major phase, and it is impossible to detect the formation of small volume fractions of α due to decomposition of the β-phase. As a consequence, the TTT-diagram given here shows only the formation of the β- and ω-phases.

2. Experimental method and results

The specimens for this study came from a commercially produced Zr–2.5 wt%Nb pressure tube. The ingot analysis of this tube showed that the major impurities were 1100 ppm O, 550 ppm Fe and 230 ppm C by weight. The billet was water-quenched from 1050 °C and extruded at 820 °C with an extrusion ratio of 10.2:1 [4]. The tube was then cold-worked 26.2% to a wall thickness of about 4 mm, but was not autoclaved. Small coupons, typically <1 cm^2, were cut from the tube (at about 0.5 m from the front-end of the extrusion) to expose radial- and longitudinal-normal (RN and LN) surfaces. The coupons were then heated for various times at selected temperatures between 400 °C and 600 °C, chemically polished with a solution of 45% HNO_3, 45% lactic acid ($C_3H_6O_3$), and 5% HF, and examined by XRD using a Rigaku rotating-anode generator operating at 12 kW with Cu Kα radiation.

* Corresponding author.
E-mail address: griffithsm@aecl.ca (M. Griffiths).

0022-3115/$ - see front matter Crown Copyright © 2008 Published by Elsevier B.V. All rights reserved.
doi:10.1016/j.jnucmat.2008.08.003

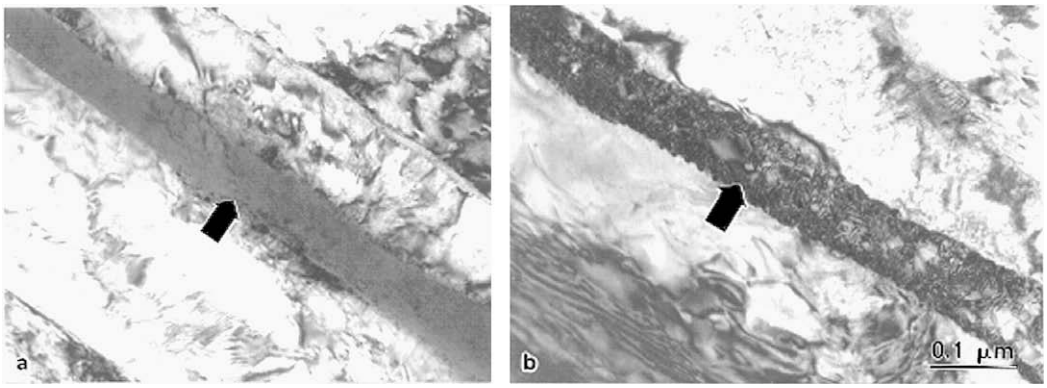

Fig. 1. Electron micrographs showing the state of the β-phase (arrowed): (a) prior to, and (b) after autoclaving of extruded and cold-drawn Zr–2.5 wt%Nb pressure tubes.

The texture of the β-phase in cold-worked Zr–2.5 wt%Nb pressure tubes is such that the (1 1 0) and (2 0 0) reflections are strongest in the LN and RN specimens, respectively, Fig. 2. The RN specimen is also useful for detecting the (2 0 1) reflection from the ω-phase.

The composition of the β-phase was obtained from a calibration of lattice parameter against Nb content from measurements on a bulk Zr–20 wt%Nb and pure Nb (99.8% purity) and assuming conformity to Vegard's Law. Measurements on pressure tube samples heated at temperatures between 400 °C and 600 °C for times up to 10000 h were then obtained and a TTT-diagram was compiled from the results.

TTT-diagrams for the Zr–19 wt%Nb alloy [3] and for the β-phase of the Zr–2.5 wt%Nb pressure tube are shown in Figs. 3(a) and (b), respectively. As noted earlier, the α-phase is excluded from the latter diagram, Fig. 3(b). The transformation behaviour shown in Fig. 3(b) differs from that in the earlier study shown in Fig. 3(a). Although only one type of Nb-enriched β-phase (referred to as β ENR in Fig. 3b) was observed in the earlier work, two types of Nb-enriched β-phase were observed in the current study for temperatures between about 425 °C and 600 °C. After long heat-treatments, the lower of the two Nb-enriched β-phases disappeared, leaving the higher Nb content phase, which eventually becomes the equilibrium β-Nb phase identified previously (Fig. 3(a)). As the transforming β-phase approaches equilibrium, it changes morphology from a filament to discrete Nb-rich precipitates [6]. At lower temperatures (400 °C) the ω-phase gradually disappears, presumably by transforming to α-phase. Where two numbers are shown within brackets, these are differing estimates of the %Nb in the β-phase using the β(1 1 0) and β(2 0 0) reflections obtained from LN and RN specimens, respectively. These differences probably result from interphase or intergranular stresses [5].

Energy dispersive X-ray analysis in a transmission electron microscope has shown that the true composition lies between the two values for β(1 1 0) and β(2 0 0) [6], and is consistent with the residual interphase stresses that are compressive in the radial direction and tensile in the longitudinal direction. The differences between the lattice parameter measurements for β(1 0 0) and β(2 0 0) eventually disappear after 1000 h at 575 °C, Fig. 3(b), presumably because the intergranular or interphase stresses have been relieved. There were no significant effects of impurities on the TTT-characteristics of Zr–2.5Nb pressure tubes for Fe content between 0.01 and 0.30 wt%, and (C + O) content between 0.11 and 0.14 wt%. Nb-enrichment did occur slightly faster in lower Fe content material after 1 h at 550 °C but had no pronounced effect on the Nb-concentration in the β-phase after 10 h of heat-treatment, Table 1.

3. Discussion

The results show that the TTT-diagram for the β-phase in the Zr–2.5 wt%Nb pressure tube differs from that of the bulk Zr–19 wt%Nb alloy in three main respects: (i) the upper limit for ω-phase formation is about 475 °C, not 525 °C; (ii) there are two metastable β-phases enriched in Nb (β, and β_2) that form at temperatures between 450 °C and 600 °C, and (iii) at temperatures >500 °C, the rate of formation of the Nb-enriched β-phases is more rapid than for the bulk material. The effects of Nb-content, microstructure, and impurities in the two materials are discussed.

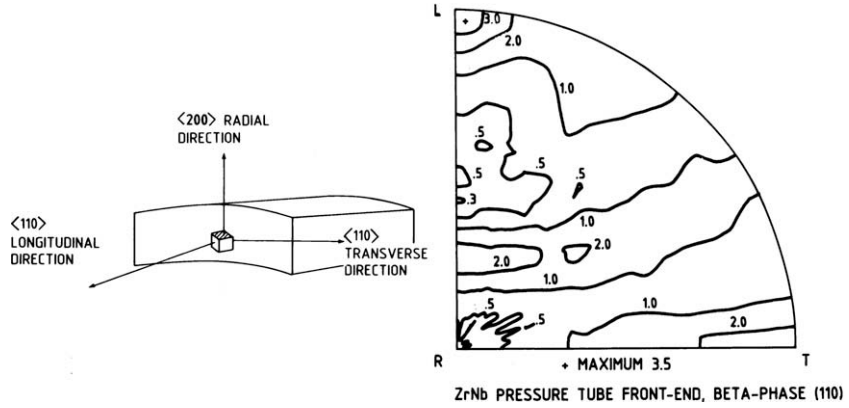

Fig. 2. Quarter (1 1 0) pole figure and schematic diagram illustrating preferred orientation of the β-phase in Zr–2.5 wt%Nb pressure tubes.

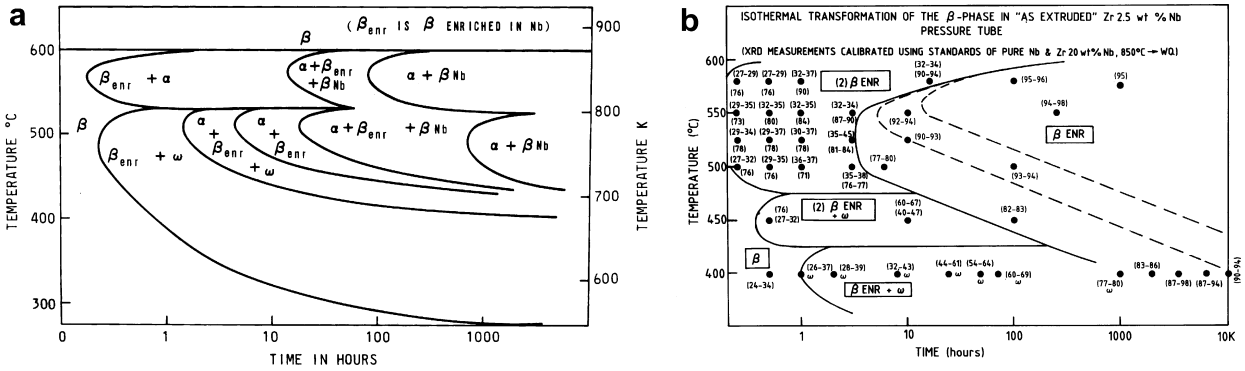

Fig. 3. (a) TTT-diagram for a Zr–19 wt%Nb alloy [2]. (b) TTT-diagram for a Zr–2.5 wt%Nb pressure tube. The numbers in brackets refer to Nb concentration. For two discrete β-phase components there are two bracketed values. Where two numbers are shown in one bracket the values refer to measurements using the (1 1 0) and (2 0 0) planes, see text.

Table 1
Nb content (wt%) measured using (2 0 0) planes as a function of heat-treatment time at 550 °C in Zr–2.5 wt%Nb pressure tubes

Tube label	Fe content (wt%)	Nb concentration (wt%) at 550 °C	
		1 h	10 h
B	0.017	$\beta_1 = 37$, $\beta_2 = 88$	$\beta_2 = 92$
C	0.017	$\beta_1 = 37$, $\beta_2 = 80$	$\beta_2 = 92$
AA	0.157	$\beta_1 = 34$	$\beta_2 = 92$
BB	0.158	$\beta_1 = 34$, $\beta_2 = 80$	$\beta_2 = 92$

3.1. Effect of Nb-content

The transformation behaviour of the bulk alloy (19 wt%Nb) could differ from that of the β-phase in a pressure tube (20–26 wt%Nb, as measured by XRD). Studies by Hehemann [7], Cheadle and Aldridge [3], and Griffiths et al. [6] indicate that increased Nb-content in the β-phase results in a decrease in the rate of enrichment, and an increase in the time required for the onset of ω-phase formation. This study, however, shows that the rate of enrichment in pressure tubes is faster than in the Zr–19 wt%Nb bulk alloy at temperatures >500 °C, even though the Nb-content is slightly higher in the β-phase of the pressure tube. In addition, the onset of ω-phase formation occurs at about the same time in both materials, suggesting that the onset of ω-phase formation is not significantly altered by slight variations in the Nb-content of the β-phase.

3.2. Effect of microstructure

It is possible that the high dislocation density introduced during the final cold-working of the pressure tubes enhances the rates of transformation of the β-phase. However, comparison between an as-extruded and an as-extruded + cold-worked tube shows that there is no significant effect on the stability of the ω-phase and on the formation of two β-enriched β-phases. Although the rate of Nb-enrichment appears to be enhanced by about 10% in the cold-worked case, it is not possible to draw any conclusions from this measurement, because of the effect of increased intergranular stresses on the lattice parameters. Residual stresses present in the dual-phase structure could be important if there were stress-enhanced transformations of the type responsible for the α-phase texture generated during high-temperature extrusion [4]. Apart from this, there is no clear indication that intergranular stresses should lower the upper temperature limit for ω-phase formation ((i) above), because one might expect stresses to promote ω-phase formation rather than suppress it [8]. The remaining feature that can be considered is β-phase morphology, and one can explain the differences outlined above as follows:

(a) The discrepancy in the temperature dependence of ω-phase formation may be explained by the morphology of the thin β-filaments in the pressure tube material. If one considers the changes at 500 °C, the ω-phase is not detected by either XRD or TEM (transmission electron microscopy) analysis in the material heat-treated for 1 h at 500 °C (Fig. 4). However, if the material is given an intermediate heat-treatment of 1 h at 700 °C (to coarsen the β-phase) prior to the treatment of 1 h at 500 °C, ω-phase formation is detected by XRD and TEM. The ω-phase is depleted in Nb and Fe [6], Fig. 5. There is no significant change in the composition of the β-phase after the heat-treatment for 1 h at 700 °C that could account for the enhancement of ω-phase formation. The stability of the β-phase in this latter case can be explained by the presence of a zone denuded of ω-phase close to the α/β interface. This denuded zone may be the result of a lowering of the vacancy supersaturation near boundaries [8]. The lower vacancy concentration close to the boundary limits the diffusion-assisted nucleation of the precipitates that one normally expects in an isothermal transformation of the type described here. The denuded zone will increase with increasing temperature, and is likely to be a limiting factor for ω-phase formation when the β-filaments are thin, as in the case of Zr–2.5Nb pressure tube material.

(b) The formation of two metastable β-phases enriched in Nb (β_1 and β_2) in the pressure tube material may also be explained in terms of the β-filament morphology. Some Nb-enrichment occurs in the β-phase filaments due to ω-phase formation (a hcp Zr-rich phase), and accounts for a

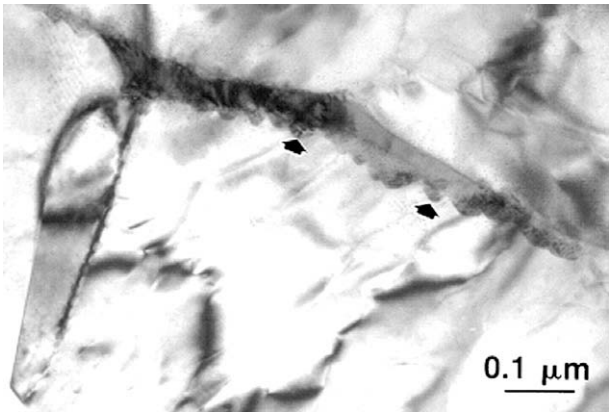

Fig. 4. Electron micrograph showing β-phase filament in pressure tube H737 after heat-treatment for 1 h at 500 °C. There is no evidence for ω-phase, although some Nb-rich precipitates are observed at the α/β interface (arrowed).

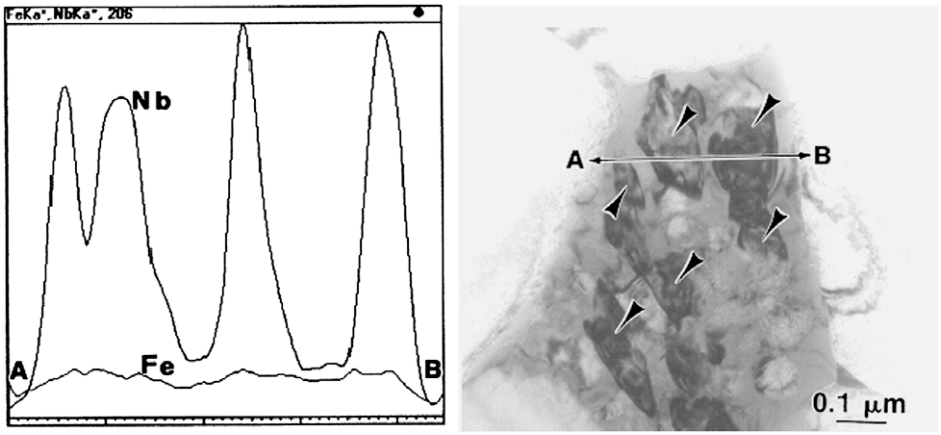

Fig. 5. Micrograph and composition profile for β-phase in Zr–2.5 wt%Nb after heating for 1 h at 700 °C and then for 1 h at 500 °C. There is a denuded zone of ω-phase particles (arrowed) at the α/β interface. The ω-phase is depleted, and the β-phase is enriched, in Nb and Fe.

general low level of enrichment. However, the ω-phase formation cannot account for the two-component β-phase structure, especially at the higher temperatures (500–600 °C), where ω-phase formation does not occur. Nb-rich precipitates are observed at the α/β-interfaces for heat-treatments corresponding to the two β-phase regions, Fig. 4. As a result, one has two-components of β-phase: one a Nb-rich precipitate at the α/β-interface and the other corresponding to the untransformed (or, at best, slightly enriched) β-phase. For a heat-treatment of 1 h at 450 °C, Nb-rich precipitates are also observed along the interface of the β-phase filaments, the filaments themselves showing evidence of internal decomposition due to ω-phase formation and therefore some enrichment of the remaining β-phase. Nb-enrichment has been observed at the α/β-interface after heat-treatment at 400 °C [6], Fig. 6, but does not appear as a second component of β-phase in the XRD analysis, probably because the volume fraction is too small in this case for detectability.

Variability in the degree or rate of decomposition of the β-phase filaments is also observed in the two-component range, especially at higher temperatures. Fig. 7 shows a typical β-phase structure in material heat-treated for 1 h at 550 °C. Some filaments remain intact (β_1) and some are completely decomposed (β_2). Therefore, a combination of variability in decomposition rate and nucleation of Nb-rich phases at the α/β interfaces can explain the formation of a two-component β-phase structure compared to the more uniform transformation for the bulk material. The β_1 and β_2 components described here are distinct from the phases reported elsewhere [9,10], for quenched and aged materials. In the latter cases the Nb-rich precipitates were equilibrium phases at the aging temperature formed from aging α-phase supersaturated with Nb. In the current work the precipitates correspond to different stages of decomposition of the metastable β-phase starting from the monotectoid composition that exists after extrusion.

(c) The β-phase morphology could also account for the more rapid formation of Nb-enriched β-phases on heating between 500 °C and 600 °C, nucleation of Nb at the α/β interface being more rapid than enrichment, due to precipitation in the bulk material.

3.3. Effect of impurities

Although we are considering the transformation behaviour of a binary alloy, the role of impurities must be considered, especially when the impurity content can be as high as 0.3 wt%, as is the case for Fe (this translates into a concentration in the β-phase of about 3 wt%). Oxygen content varies less than Fe content; in actual fact, the oxygen in pressure tubes is a required addition for increased

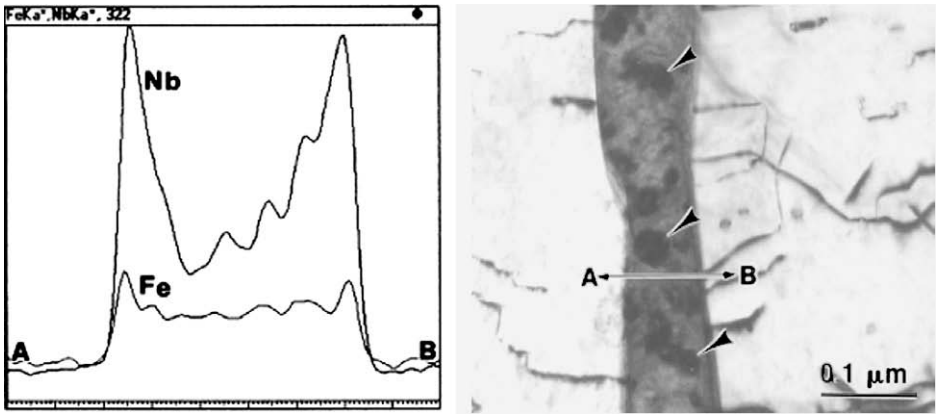

Fig. 6. Micrograph and composition profile for β-phase in Zr–2.5 wt%Nb after heating for 24 h at 400 °C. The filaments contain ω-phase particles (arrowed) and there is segregation of Nb and Fe at the α/β interface.

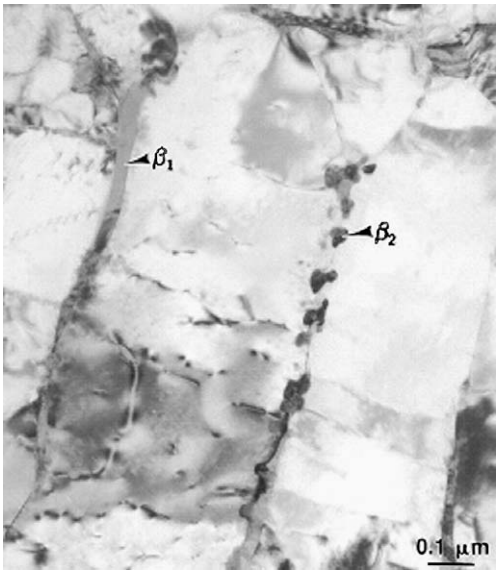

Fig. 7. Electron micrograph showing the state of the β-phase in pressure tube H737 after heat-treatment for 1 h at 550 °C. Nb-rich precipitates are formed at the α/β interface or form completely decomposed (discontinuous) β-phase (β_2). Other segments of β-phase remain relatively intact (β_1).

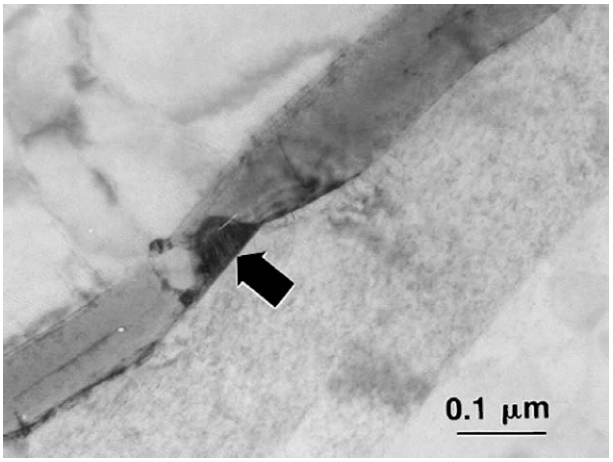

Fig. 8. Electron micrograph showing a β-phase filament containing an Fe-rich precipitate (arrowed) in pressure tube H737 after heating for 1 h at 550 °C.

strength and is typically about 0.12 wt%. Iron is simply an impurity and ranges from about 0.05 wt% to 0.15 wt% for most tubes.

The two impurities O and Fe have opposite effects in terms of the phase diagram; oxygen is an α-stabiliser and Fe is a β-stabiliser. Oxygen in particular has a marked effect, as it increases the α + β/β transus temperature [11]. One might expect that Fe would have the opposite effect. There is little data to show the effect of O and Fe on the monotectoid temperature, although work on pressure tube materials shows that the monotectoid temperature is 590 °C [12], and not 610 °C for the Zr–Nb binary diagram of Lundin and Cox, [1]. This was confirmed in the present work from heat-treatments at 600 °C, after which the β-phase composition reverts back to the nominal monotectoid composition. One might attribute the lower monotectoid temperature for pressure tubes to the presence of more Fe or less O, compared with the material used to derive the earlier phase diagram [1]. Work by Bethune and Williams indicated that the phase diagram most applicable to Zr–2.5Nb pressure tubing was that due to Richter et al. [14]. This has been confirmed in the current study by establishing that the α + β/α transus for Zr–2.5Nb occurs at about 595 °C.

There is no consensus about the precise monotectoid composition. The best that can be said is that it is >17 wt%Nb [12,13]. If one looks at the microstructure of the Zr–19 wt%Nb alloy used by Aldridge and Cheadle [2,3] it appears that some other second phase (possibly α-phase) has formed, and it is therefore conceivable that the monotectoid composition for their alloy was >19 wt%Nb. In addition, we have examined nominal 20 wt%Nb material slow-cooled from the (α + β)-phase and have observed α-grains, indicating that the monotectoid composition may, in fact, be >20 wt%Nb. XRD data using a quenched 20 wt%Nb alloy as a standard show that the Nb concentration in the β-phase is between 20 wt%Nb (110) and 26 wt%Nb (200) for an as-extruded and cold-worked pressure tube. This is consistent with the value of about 21 wt%Nb obtained from TEM analysis, see Section 3.4.

Although impurities can affect the phase diagram, there is little evidence in the present work that Fe or O in the range of 0.05–0.15 wt% has any significant effect on the transformation kinetics of the β-phase below the monotectoid temperature. As Fe is a β-stabiliser, one might have expected to see some effect in the transformation kinetics for low and high Fe content. However, because Fe is a rapid diffuser, it quickly precipitates during heat-treatment, forming an Fe-rich layer at the α/β interface at low temperatures, Fig. 6, or discrete precipitates at higher temperatures, Fig. 8. Therefore, the Fe could only significantly affect the transformation kinetics in the early stages of heat-treatment, as observed (Table 1).

3.4. Comparison with TEM data

The accuracy of the XRD analysis is only as good as the standards used and the method of extrapolation. Rodgers and Atkins [15] have shown that Nb in solution obeys Vegard's law; i.e., the lattice parameter is inverse linearly proportional to the Nb concentration. In this respect the calibration method used here is valid, although slight errors might exist because only two standards are used (20 wt%Nb and 99.8 wt%Nb) and, in addition, there may be impurity variations that alter the lattice parameters.

The accuracy of the XRD data was compared with EDX-analysis using a TEM. Using the quenched 20 wt%Nb alloy as a standard, EDX-analysis showed that the composition of the β-phase in the as-received pressure tube material was 21.3 ± 1.8 wt%Nb [6]. This compares well with the XRD data giving 20 wt% (110)–26 wt% (200). For fully transformed material, however, a discrepancy existed with the TEM data, giving 88.0 ± 3.1 wt%Nb, compared with 95 wt%Nb from the XRD data. The EDX-analysis underestimates the XRD data by about 8% in each case. The discrepancy may be accounted for in terms of the effect of stress on the XRD measurements; dilatational components could exist even when the deviatoric components are relaxed. Differences in purity between the standards and actual pressure tube material and deviations from Vegard's Law could also affect the results.

The ZrNbFe-rich precipitates formed by decomposition of the β-phase are not in sufficient volumes to be detectable by XRD analysis. EDX measurements are ambiguous concerning their composition – either $(Zr,Nb)_3Fe$ or $Zr(Nb,Fe)_2$ depending on whether the Fe is associated with the Zr or Fe.

4. Conclusions

A TTT-diagram has been derived for Zr–2.5Nb pressure tubes. Apart from the insensitivity to changes in the α-phase volume fraction, there are differences between this and previous work on a bulk β-phase material that can mostly be attributed to the morphology of the β-phase, the width and number of the α/β interfaces

being a significant factor in determining the transformation characteristics of the pressure tube materials.

References

[1] C.E. Lundin, R.H. Cox, USAEC Report No. 1/At(11-1)-752, 1960.
[2] S.A. Aldridge, B.A. Cheadle, J. Nucl. Mater. 42 (1972) 32.
[3] B.A. Cheadle, S.A. Aldridge, J. Nucl. Mater. 47 (1973) 255.
[4] R.A. Holt, S.A. Aldridge, J. Nucl. Mater. 135 (1985) 246.
[5] M. Griffiths, J.F. Mecke, J.E. Winegar, T.M. Holden, R.A. Holt, Adv. X-ray Anal. 35 (1992) 475.
[6] M. Griffiths, C.K. Chow, C.E. Coleman, R.A. Holt, S. Sagat, V.F. Urbanic, ASTM STP 1175 (1993) 1077.
[7] R.F. Hehemann, Can. Met. Quart. 11 (1972) 201.
[8] D. de Fontaine, Met. Trans. A. 19A (1988) 169.
[9] S. Banerjee, S.J. Vijayakar, R. Krishnan, J. Nucl. Mater. 62 (1976) 229.
[10] C.P. Luo, G.C. Weatherley, Metall. Trans. A. 19A (1988) 1153.
[11] C.E.L. Hunt, P. Niessen, J. Nucl. Mater. 35 (1970) 134.
[12] I.T. Bethune, C.D. Williams, AECL-2715 (1968).
[13] J.P. Abriata, J.C. Bolcich, Bull. Alloy Phase Diagram 3 (1982) 34.
[14] H. Richter, P. Wincierz, K. Anderko, U. Zwicker, J. Less Common Metals 4 (1962) 252.
[15] B.A. Rodgers, D.F. Atkins, Trans. AIME 203 (1955) 1034.